

Serotonin 5-HT_{1A}, 5-HT_{2A} and dopamine D₂ receptors strongly influence prefronto-hippocampal neural networks in alert mice: Contribution to the actions of risperidone

Abbreviated title: Antipsychotic modulation of neural networks

Thomas Gener^{1,*}, Adrià Tauste-Campo^{2,3,*}, Maria Alemany-González¹, Pau Nebot¹, Cristina Delgado-Sallent¹, Jordi Chanovas^{1,&}, M. Victoria Puig¹

¹ Integrative Pharmacology and Systems Neuroscience, Hospital del Mar Medical Research Institute, Barcelona Biomedical Research Park, 08003 Barcelona, Spain

² Barcelonaβeta Brain Research Center, Pasqual Maragall Foundation, 08005 Barcelona, Spain

³ Centre for Brain and Cognition, University Pompeu Fabra, 08018 Barcelona, Spain

* These authors contributed equally

& Present address: SUNY Downstate Medical Center, 11203 New York, NY, United States

Corresponding author: M. Victoria Puig. Email: mpuig3@imim.es. Office Phone: +34 933160482

Number of figures and tables: 7 figures, 2 tables

Supplementary information: Text and 4 figures

The authors declare no competing financial interests.

Abstract

Atypical antipsychotic drugs (APDs) used to treat positive and negative symptoms in schizophrenia block serotonin receptors 5-HT_{2A}R and dopamine receptors D₂R and stimulate 5-HT_{1A}R directly or indirectly. However, the exact cellular mechanisms mediating their therapeutic actions remain unresolved. We recorded neural activity in the prefrontal cortex (PFC) and hippocampus (HPC) of freely-moving mice before and after acute administration of 5-HT_{1A}R, 5-HT_{2A}R and D₂R selective agonists and antagonists and atypical APD risperidone. We then investigated the contribution of the three receptors to the actions of risperidone on brain activity via statistical modeling and pharmacological reversal (risperidone + 5-HT_{1A}R antagonist WAY-100635, risperidone + 5-HT_{2A/2C}R agonist DOI, risperidone + D₂R agonist quinpirole). Risperidone, 5-HT_{1A}R agonism with 8-OH-DPAT, 5-HT_{2A}R antagonism with M100907, and D₂R antagonism with haloperidol reduced locomotor activity of mice that correlated with a suppression of neural spiking, power of theta and gamma oscillations in PFC and HPC, and reduction of PFC-HPC theta phase synchronization. By contrast, activation of 5-HT_{2A}R with DOI enhanced high-gamma oscillations in PFC and PFC-HPC high gamma functional connectivity, likely related to its hallucinogenic effects. Together, power changes, regression modeling and pharmacological reversals suggest an important role of 5-HT_{1A}R agonism and 5-HT_{2A}R antagonism in risperidone-induced alterations of delta, beta and gamma oscillations, while D₂R antagonism may contribute to risperidone-mediated changes in delta oscillations. This study provides novel insight into the neural mechanisms for widely prescribed psychiatric medication targeting the serotonin and dopamine systems in two regions involved in the pathophysiology of schizophrenia.

Keywords: schizophrenia; antipsychotic drug; prefrontal cortex; hippocampus; neural synchronization; *in vivo* electrophysiology

Highlights

- 5-HT_{1A}R agonism and 5-HT_{2A}R/ D₂R antagonism inhibit prefronto-hippocampal network activity.
- 5-HT_{2A}R activation enhances cortical and circuit synchronization at high gamma frequencies.
- Risperidone reduces prefronto-hippocampal activity via 5-HT_{1A}R, 5-HT_{2A}R and D₂R activities.
- 5-HT_{1A}R, 5-HT_{2A}R and D₂R may contribute to sedation by risperidone.

1. Introduction

The prefrontal cortex (PFC) and hippocampus (HPC) are essential in mediating numerous behavioral and cognitive processes. Interactions between the two structures also contribute to behavior and are disrupted in psychiatric disorders (Sigurdsson and Duvarci, 2016). Both regions are highly innervated by serotonergic afferents originating in the midbrain raphe nuclei (Groenewegen and Uylings, 2000; Hensler, 2006) and densely express serotonin 5-HT_{1A} and 5-HT_{2A} receptors (5-HT_{1A}R and 5-HT_{2A}R) (Berumen et al., 2012; Celada et al., 2013). In addition, they express moderate levels of dopamine D₂ receptors (D₂R) (Puighermanal et al., 2015; Santana et al., 2009). 5-HT_{1A}R and 5-HT_{2A}R strongly influence PFC and HPC neural activity. We have previously shown that pharmacological activation of 5-HT_{1A}R decreases neural spiking and gamma oscillations (30-80 Hz) in the PFC of anesthetized rodents whereas activation of 5-HT_{2A}R exerts the opposite effect (Puig et al., 2010). This is consistent with the inhibitory and excitatory postsynaptic transmission mediated by 5-HT_{1A}R and 5-HT_{2A}R, respectively (Celada et al., 2013). In HPC, serotonin regulates theta oscillations (4-8 Hz) via 5-HT_{1A}R (Kocsis et al., 2006; Vertes et al., 1994). Moreover, D₂R can increase or decrease spiking activity *in vivo* in both structures (Gee et al., 2012; Lavin et al., 2005; Puig and Miller, 2015). However, a comprehensive characterization of 5-HT_{1A}R, 5-HT_{2A}R and D₂R influences on neural activity of the PFC and HPC and PFC-HPC functional connectivity *in vivo* is missing. This is a challenging task as the serotonin and dopamine systems interact with each other (Bortolozzi et al., 2010), the two serotonin receptors are expressed by excitatory and inhibitory neurons (Celada et al., 2013) and are highly co-expressed in pyramidal neurons of the PFC (Amargós-Bosch et al., 2004).

The PFC and HPC display anatomical and functional abnormalities in patients with schizophrenia that contribute to the severe symptoms associated with the disorder (Heckers and Konradi, 2010; Minzenberg et al., 2009). Atypical APDs such as risperidone (RIS) and clozapine, that produce less extrapyramidal side effects than typical APDs, block extensively 5-HT_{2A}R and stimulate directly or indirectly 5-HT_{1A}R. In fact, 5-HT_{1A}R and 5-HT_{2A}R are major targets for antipsychotic drugs (APDs) that have proven useful to treat psychosis and cognitive impairment in schizophrenia (Meltzer and Huang, 2008; Roth et al., 2004). By contrast, typical APDs like haloperidol (HAL) are mainly dopamine D₂R antagonists and bind weakly to

serotonin receptors (Meltzer and Massey, 2011; Meltzer and Huang, 2008). Notably, RIS also acts as a D₂R antagonist, so an interaction between the serotonin and dopamine systems may be essential for some APD therapeutic actions (Wang et al., 2018). APDs bind to other targets outside the serotonin and dopamine systems including histaminergic, adrenergic, and muscarinic receptors. Behaviorally, many APDs have sedative effects on patients. Sedation is a state of drowsiness that has been attributed to dosage and affinity for histamine H₁ receptors. Not all antipsychotic medications have the same sedative effect and atypical APDs cause less sedation compared with conventional APDs (Miller, 2004). Yet, atypical APDs are as effective in controlling psychosis in schizophrenia patients as typical APDs while producing some cognitive amelioration that has been partly attributed to 5-HT_{1A}R agonism and 5-HT_{2A}R antagonism (Meltzer et al., 2012; Roth et al., 2004). The neurophysiological mechanisms mediating these effects may involve gamma oscillations, as atypical APDs reduce excessive gamma power (50-100 Hz) in the EEG of schizophrenia patients and rodent models of schizophrenia (Ahnaou et al., 2017; Jones et al., 2012; Uhlhaas and Singer, 2010).

Here, we investigated how selective pharmacological activation and inhibition of 5-HT_{1A}R, 5-HT_{2A}R and D₂R influence PFC and HPC neural activity and PFC-HPC phase synchronization in freely-moving mice and compared their actions with those of atypical APD RIS. We further investigated the potential contributions of 5-HT_{1A}R agonism, 5-HT_{2A}R and D₂R antagonism to the effects of RIS by independently using linear regression modeling and pharmacological reversal.

2. Materials and methods

2.1. Animals

C57BL/6 male mice (n = 22) were obtained from the local colony at the Barcelona Biomedical Research Park (PRBB) Animal Facility. All procedures were authorized by the Animal Research Ethics Committee (PRBB-CEEA) and the Catalan government and were carried out in accordance with the guidelines of the European Union Council (EU Directive 2010/63/EU) and Spanish regulations (BOE 252/34367-91, 2005). Mice were 2 to 3 months old at the start of the experiments and weighed between 20 to 30 g. Animals were

housed in a 12-h light-dark cycle schedule from 8 am until 8 pm and received the standard pellet diet provided by the animal facility throughout the experiment.

2.2. Surgeries

Mice were induced with a mixture of ketamine/xylazine and placed in a stereotaxic apparatus. Anesthesia was maintained with continuous 0.5-4% isoflurane. Small craniotomies were drilled above the medial PFC and HPC. Several micro-screws were placed into the skull to stabilize the implant, and the one on top of the cerebellum was used as a general ground. Three tungsten electrodes, one stereotrode and one single electrode, were implanted in the PFC and three more were implanted in the HPC. The electrodes were positioned stereotaxically in the prelimbic PFC (AP: 1.5, 2.1 mm; ML: \pm 0.6, 0.25 mm; DV: -1.7 mm from bregma) and in the CA1 area of the HPC (AP: -1.8, -2.5 mm; ML: -1.3, -2.3 mm; DV: -1.15, -1.25 mm). In addition, three reference electrodes were implanted in the corpus callosum and lateral ventricles (AP: 1, 0.2, -1; ML: 1, 0.8, 1.7; DV: -1.25, -1.4, -1.5, respectively) (Fig. 1A). Half of the animals had the electrodes implanted in the right hemisphere and the other half in the left hemisphere. The electrodes were made by twisting a strand of tungsten wire 25 μ m wide (Advent, UK), had impedances that ranged from 100 to 400 kOhm at the time of implantation and were implanted unilaterally with dental cement. Electrode wires were pinned to an adaptor to facilitate their connection to the recording system. After surgery animals were allowed at least one week to recover during which they were extensively monitored and received both analgesia and anti-inflammatory treatments. Additionally, animals were handled and familiarized with the implant connected to the recording cable. After the experiments ended, the electrode placements were confirmed histologically by staining the brain slices using Cresyl violet (Fig. 1B). Electrodes with tips outside the targeted areas were discarded from data analyses.

2.3. Neurophysiological recordings and data analyses

Electrophysiological recordings were carried out in freely-moving mice exploring their home cages (369 x 165 x 132 mm with standard bedding) with the multi-channel Open Ephys system at 0.1-6000 Hz and a sampling rate of 30 kHz with Intan RHD2132 amplifiers equipped with an accelerometer. The home cage was moved from the housing room to the experimental room within the animal facility where recordings were implemented. The recording room was located in the SPF area of the animal facility where

environmental and electrical noise was kept to a minimum. Electrophysiological recordings were typically implemented during the morning hours (from 10h to 13h) for 2 or 3 hours depending of the experimental protocol. Two to three animals were recorded simultaneously in separate cages and electrophysiological setups in the same room separated by partitions. Animals did not have access to food or water during the recording sessions but had food and water available just before and after each experiment. All the recordings were carried out during the light cycle of housing. The lighting conditions were monitored to be between 8-15 luxes.

We used the accelerometer's signals in the x, y and z axis to evaluate the effects of the drugs on general mobility of mice. We found that the variance of the acceleration module (Acc),

$$Acc = \text{Variance} (\sqrt{ax^2 + ay^2 + az^2})$$

which quantifies the variation of movement across the three spatial dimensions, was maximum during exploration and decreased as the animals were in quiet alertness, natural sleep or sedation (Fig. 1C). More specifically, raw x, y and z signals were first downsampled to 1 kHz, then we calculated the instantaneous module from which we measured the variance of 1 minute bins (Supplementary Fig. 1). In addition, recorded signals from each electrode were filtered offline to extract multi-unit activity (MUA) and local field potentials (LFPs). MUA represents an aggregate signal reflecting local spiking activity and was estimated by first subtracting the raw signal from each electrode with the signal from a nearby referencing electrode (Fig. 1A) to remove artifacts related to the animal's movement. Then, continuous signals were filtered between 450-6k Hz with Python and thresholded at -3 sigma standard deviations with Offline Sorter v3 (Plexon Inc.) (Mattia et al., 2010; Stark and Abeles, 2007). Noise was removed using principal component analysis and action potentials from different neurons (i.e., with different shapes) were quantified during the time windows of analysis (typically 10 min) and provided as spikes per second. To obtain LFPs, signals were downsampled to 1 kHz, detrended and notch-filtered to remove noise line artifacts (50 and 100 Hz) with custom-written scripts in Python. Signals were then bandpass filtered at 1-250 Hz. Power density and spectrograms were constructed using the multi-taper method in MATLAB with the Chronux toolbox (Bokil et al., 2010). The taper parameters chosen for the analyses were: 9 tapers, 0.17 Hz bandwidth, 30 s sliding time window

[params.tapers = (5,9), 1–100 Hz range, no padding]. The frequency bands considered for the band-specific power analyses included delta (3-5 Hz), theta (8-10 Hz), beta (15-25 Hz), low gamma (30-50 Hz), and high gamma (50-100 Hz). Corrected estimations of power were obtained by multiplying the original multi-taper estimation by the frequency to compensate for the 1/f power decay. PFC-HPC functional connectivity was estimated via the phase-lag index (PLI, Butterworth filter of order 3), a measure of phase synchronization between areas aimed at removing the contribution of common source zero-lag effects to the overall synchronization value. That is, the PLI allowed us to estimate the synchronization between the PFC and the HPC mitigating source signals affecting multiple regions simultaneously (Hardmeier et al., 2014; Stam et al., 2007; Vinck et al., 2011). Results (Acc, MUA, LFP power, PFC-HPC PLI) are provided as z-scores with respect to baseline statistics (i.e., data is demeaned by the baseline mean and then normalized by the baseline standard deviation).

2.4. Pharmacology

8-hydroxy-2-(di-n-propylamino)tetraline (8-OH-DPAT) (DPAT, 5-HT_{1A}R agonist), 1-(2,5-dimethoxy-4-iodophenyl)-2 amino propane (DOI, partial 5-HT_{2A/2C}R agonist), M100907 (5-HT_{2A}R antagonist), quinpirole (QUI, D_{2/3}R agonist), haloperidol (HAL, D_{2/3}R antagonist and typical APD), and risperidone (RIS, atypical APD) were obtained from Sigma/Aldrich. WAY-100635 (WAY, 5-HT_{1A}R antagonist) was obtained from Biogen Científica. Doses were: DPAT and DOI, 0.3 and 1 mg/kg; M100907 and quinpirole 1 mg/kg; WAY-100635 and haloperidol 0.5 mg/kg; RIS 2 mg/kg. These are low to medium doses in mice that were chosen based on previous studies (Adem et al., 2019; Bortolozzi et al., 2012; Brookshire and Jones, 2009; Egashira et al., 2007; Wu et al., 2017). All drugs were administered intraperitoneally (I.P.). Each mouse was used to test multiple drugs and at least one week of washout was left between each experiment.

2.5. Experimental design and statistical analyses

All experiments consisted of 30 minutes baseline period, 30 minutes following administration of saline, 1 hour period following administration of the first drug (agonists and antagonists), and 1 hour period following administration of the second drug (antagonists following agonists only) (Fig. 1D). In experiments that aimed to reverse the effects of RIS, the second drug (WAY, DOI, QUI) was administered 30 minutes after RIS. An experimental group where only saline was injected was used as general control. Two-way mixed ANOVA

was used to test for statistical significance with time as within subject factor (baseline, saline, drug 1 and drug 2 or baseline, saline and drug 1 samples when appropriate) and treatment as between subject factor (saline vs. drug of interest) for Acc, MUA, LFP power and PFC-HPC PLI with IBM SPSS Statistics software (PASW Statistics 18). Drug effects were quantified in 10 min periods (last 10 min of baseline and saline, and minutes 25-35 after drug injections). Raw data (not z-scores) were used in all statistical analyses. We corrected for the use of mice in multiple experiments adding a random factor in the ANOVAs and used the Bonferroni method to adjust for multiple comparisons.

2.6. Linear regression models

We considered three main statistical models per electrode to independently estimate the linear association between the regressors DPAT (5-HT_{1A}R agonism), M100907 (5-HT_{2A}R antagonism) and haloperidol (D₂R antagonism), and the regressand RIS (Model 1: RIS vs. DPAT, n = 5 mice, n = 10 electrodes; Model 2: RIS vs. M100907, n = 5 mice, n = 15 electrodes; Model 3: RIS vs. HAL, n = 5 mice, n = 10 electrodes), in z-scored band-specific LFP power recorded from PFC and HPC during the first hour after drug injection (power estimation window = 60 s, n = 58 model time samples). In addition, we used a model with saline to assess the specificity of our results (Model 4: RIS vs. saline, n = 4 mice, n = 11 electrodes). The models were fed with paired data recordings (RIS and drug/saline) from the same animal and electrode (see Supplementary information). In each model, we included the variance of the animal's instantaneous acceleration during the risperidone experiment as a second regressor. For all electrode-based models, we (a) computed the variance explained (VE) by both regressors (drug/saline and acceleration), and (b) estimated the partial contribution of each regressor into RIS' LFP power via the proportion of partial variance explained (PVE). The PVE of a regressor x is the reduction in prediction error that results from including x in a model where x was not present. Statistical comparisons of PVE values across different models were made using Wilcoxon Rank test. The test was double-tailed for comparison across drug components and right-tailed for comparisons with the saline model.

3. Results

3.1. Activation of 5-HT_{1A}R suppresses local activity in PFC and HPC and prefronto-hippocampal theta synchronization

We first examined whether activation of 5-HT_{1A}R with the selective agonist 8-OH-DPAT (DPAT; 1 mg/kg, n = 8 mice) and inhibition with the selective antagonist WAY-100635 (WAY; 0.5 mg/kg, n = 6 mice) affected general locomotor activity of mice and neural network activity (multi-unit activity [MUA] and local field potential [LFP] power) in the prelimbic PFC and CA1 region of the HPC of freely-moving mice. Following baseline and saline control periods (30 minute each, Fig. 1D), DPAT was administered followed by WAY one hour later. Injection of saline alone at the same time points served as the control group (n = 7 mice).

Two-way mixed ANOVA (with time as within factor and treatment [saline, DPAT-WAY] as between factor) showed that DPAT reduced animals' locomotor activity, an effect that was reversed by WAY ($F_{3,42} = 5.949$, $p = 0.002$ for time x treatment interaction), with significant post-hoc differences between saline and DPAT groups ($p = 0.001$) but not between saline and WAY groups (Fig. 2A). DPAT also reduced MUA in the PFC and HPC, an effect that was reversed by WAY (PFC: $F_{2,25} = 37.293$; HPC: $F_{3,45} = 14.983$, $p < 0.00005$) (Fig. 2B). WAY alone did not affect locomotion but decreased MUA moderately in PFC ($F_{1,18} = 4.483$, $p = 0.039$) (Fig. 2A and B). The effects of DPAT were accompanied by marked reductions of power in all frequency bands, except delta oscillations, that were unchanged. We noted though that within delta frequencies a narrow low-amplitude band of 4 Hz became visible in PFC (see below). Fig. 2C depicts representative examples of DPAT's effects on the oscillatory power recorded from individual electrodes in the PFC and HPC (upper panels) and the group's effect (z-scores, n = 8 mice; lower panels). DPAT disrupted theta, beta, and gamma oscillations in both regions ([theta] PFC: $F_{3,39} = 11.795$; HPC: $F_{3,39} = 15.782$, $p < 0.00005$; [beta] PFC: $F_{3,36} = 7.034$, $p = 0.001$; HPC: $F_{2,28} = 6.935$, $p = 0.001$; [low-gamma] PFC: $F_{3,39} = 3.8$, $p = 0.018$; HPC: $F_{2,24} = 13.196$, $p < 0.00005$; [high-gamma] PFC: $F_{3,36} = 9.467$, HPC: $F_{3,39} = 12.598$, $p < 0.00005$), while a low-amplitude 4 Hz band remained in PFC (Supplementary Fig. 2). WAY reversed these effects across all bands suggesting a selective mediation by 5-HT_{1A}R. Noteworthy, a lower dose of DPAT (0.3 mg/kg) exerted similar effects on the circuit and only reductions of MUA and low gamma power were clearly dose-

dependent (Supplementary Fig. 2). WAY alone slightly increased beta waves in the HPC ($F_{2,20} = 3.076$, $p = 0.068$ for time x treatment [saline, WAY] interaction) (Fig. 2C and D). We also investigated PFC-HPC functional connectivity via the phase-lag index (PLI), a measure that estimates phase synchronization between areas removing the effect of zero-lag interactions. DPAT reduced PFC-HPC phase synchronization at theta and beta frequencies ([theta] $F_{3,39} = 9.143$, $p < 0.00005$; ([beta] $F_{3,39} = 3.558$, $p = 0.023$) that were reversed by WAY (Fig. 2E).

In summary, 5-HT_{1A}R agonism reduced locomotor activity of mice while decreasing spiking and oscillatory activities in PFC and HPC and PFC-HPC phase synchronization, particularly at theta ranges (Table 1).

3.2. 5-HT_{2A}R activation enhances PFC high gamma and prefronto-hippocampal high gamma synchronization whereas 5-HT_{2A}R inhibition suppresses local activity in PFC and HPC and boosts delta oscillations

We next assessed the actions of the partial 5-HT_{2A/2C}R agonist and hallucinogen DOI (1 mg/kg, $n = 7$ mice) and the selective 5-HT_{2A}R antagonist M100907 (1 mg/kg, $n = 8$ mice) on mice mobility and neural network activity of the PFC and HPC following the same experimental protocol as above. DOI did not affect the animals' general locomotor activity (Fig. 3A) but caused head twitches and other behaviors associated with hallucinations in rodents (Schmid et al., 2008). Moreover, it modestly decreased MUA in the PFC ($F_{2,48} = 4.287$, $p = 0.033$ for time x treatment [saline, DOI-M100907] interaction) (Fig. 3B). Conversely, DOI selectively enhanced the power of PFC high gamma oscillations ($F_{2,19} = 8.236$, $p = 0.004$) and PFC-HPC high gamma phase synchronization ($F_{3,36} = 3.321$, $p = 0.03$ for time with no interaction) that were reversed by M100907 (Fig. 3C,D, E). This high-gamma increase was not observed in HPC, nor did alterations in other oscillatory frequencies (Table 1). A lower dose of DOI (0.3 mg/kg) exerted similar effects (Supplementary Fig. 3).

Blocking 5-HT_{2A}R with M100907 suppressed locomotor activity ($F_{2,24} = 8.195$, $p = 0.002$ for time x treatment [saline, M100907] interaction) (Fig. 3A), MUA (PFC: $F_{1,20} = 8.895$, $p = 0.005$; HPC: $F_{2,32} = 8.939$ for time with no interaction, $p = 0.001$) (Fig. 3B), and theta power (PFC: $F_{2,26} = 18.706$, $p < 0.00005$; HPC:

$F_{2,24} = 7.792$, $p = 0.002$) in both regions (Fig. 3C and D). By contrast, delta oscillations were increased (PFC: $F_{1,15} = 6.703$, $p = 0.018$; HPC: $F_{1,10} = 7.017$, $p = 0.049$), particularly at 4 Hz (Supplementary Fig. 3), as after DPAT. M100907 also decreased low and high gamma power and this effect was larger after administration of DOI (low gamma after DOI; PFC: $p = 0.005$; HPC: $p < 0.00005$). M100907 also decreased theta PFC-HPC phase synchronization (PLI) ($F_{3,30} = 8.123$, $p < 0.00005$ for time factor with no interaction) (Fig. 3E), but very modestly compared to DPAT.

3.3. Activation and inhibition of D₂R suppress local activity in PFC and HPC and enhance delta oscillations

The effects of the D₂R agonist quinpirole (QUI; 1 mg/kg, $n = 4$ mice) and antagonist haloperidol (HAL; 0.5 mg/kg, $n = 7$ mice) were also investigated on the same circuit. Quinpirole decreased animals' locomotor activity ($F_{3,30} = 13.979$, $p < 0.00005$ for time x treatment [saline, QUI-HAL] interaction) and this was partly reversed by haloperidol (quinpirole vs. saline, $p = 0.02$; haloperidol vs. saline, $p = 0.214$). Interestingly, haloperidol administration alone largely suppressed locomotor activity as well ($F_{2,26} = 5.334$, $p = 0.011$) (Fig. 4A), which most likely reflects sedation induced by the drug's antipsychotic activity (Gallitano-Mendel et al., 2008; Joshi et al., 2017). Both quinpirole and haloperidol reduced MUA in both brain structures ([QUI] PFC: $F_{2,16} = 21.557$, $p < 0.00005$; HPC: $F_{2,14} = 13.941$, $p = 0.001$; [HAL] PFC: $F_{1,19} = 15.106$, $p = 0.001$; HPC: $F_{1,20} = 3.74$, $p = 0.035$) (Fig. 4B), indicating that there is a limited range of D₂R activation for normal spiking of neurons. QUI strongly disrupted neural oscillations of the PFC and HPC. Theta, beta and high gamma oscillations were consistently decreased following quinpirole administration ([theta] PFC: $F_{1,9} = 14.059$, $p = 0.003$; HPC: $F_{3,21} = 17.246$, $p < 0.00005$; [beta] PFC: $F_{3,21} = 10.576$, $p < 0.00005$; HPC: $F_{3,21} = 13.502$, $p < 0.00005$; [high-gamma] PFC: $F_{1,9} = 5.935$, $p = 0.03$; HPC: $F_{1,8} = 4.158$, $p = 0.05$). These effects were reversed by haloperidol, indicating the participation of D₂R. Quinpirole also reduced PFC-HPC theta phase synchronization ($F_{3,18} = 8.172$, $p = 0.001$). By contrast, it increased delta oscillations in HPC ($F_{1,14} = 4.592$, $p = 0.028$) and PFC-HPC delta phase synchronization ($F_{2,9} = 9.788$, $p = 0.007$).

Haloperidol alone substantially increased delta oscillations in PFC and HPC ($F_{1,14} = 31.424$, 40.962 , $p < 0.00005$ for time x treatment [saline, HAL] interaction), including the 4 Hz band, while moderately

decreasing PFC theta power ($F_{1,16} = 5.111$, $p = 0.03$ for time without interaction). Haloperidol also produced a general suppression of gamma oscillations, particularly high gamma ([low gamma] PFC: $F_{1,15} = 15.306$, $p = 0.001$; HPC: $F_{2,22} = 12.4$, $p < 0.00005$ for time factor; [high gamma] PFC: $F_{2,24} = 12.604$, $p < 0.00005$; HPC: $F_{1,15} = 3.761$, $p = .038$ for time x treatment interaction)(Fig. 4C and D). Finally, haloperidol decreased PFC-HPC phase synchronization at theta frequencies ($F_{2,20} = 4.33$, $p = 0.027$) (Fig. 4E).

Collectively both activation and inhibition of D₂R reduced MUA, theta and high gamma oscillations in PFC and HPC supporting a fine range of D₂R activation for proper neural network function. Relevant to antipsychotic drug action, D₂R antagonism with haloperidol suppressed PFC and HPC activity and PFC-HPC theta connectivity resembling 5-HT_{1A}R activation and 5-HT_{2A}R blockade. Moreover, it markedly amplified delta waves, mimicking 5-HT_{2A}R blockade with M100907 (Table 1).

3.4. Risperidone strongly reduces PFC-HPC network activity

We next investigated the effects of the atypical APD risperidone (RIS; 2 mg/kg, n = 8 mice) on the PFC-HPC circuit. Similar to the typical APD haloperidol, RIS largely suppressed locomotor activity ($F_{2,28} = 11,145$, $p < 0.00005$ for time x treatment [saline, RIS] interaction) possibly reflecting states of sedation (Fig. 5A). Also as haloperidol, RIS consistently reduced MUA (PFC: $F_{1,25} = 34.863$, HPC: $F_{2,36} = 12.751$, $p < 0.00005$) and gamma oscillations in both regions ([high gamma] PFC: $F_{2,24} = 22.369$, $p < 0.00005$; HPC: $F_{1,16} = 6.488$, $p = 0.017$), and enhanced delta waves (PFC: $F_{1,14} = 3.929$, $p = 0.033$; HPC: $F_{1,14} = 11.546$, $p = 0.003$) (Fig. 5B-D). However, as opposed to haloperidol, RIS also disrupted theta and beta oscillations in both regions ([theta] PFC: $F_{1,14} = 15.506$, $p = 0.001$; HPC: $F_{2,26} = 16.2$, $p < 0.00005$; [beta] PFC: $F_{1,16} = 7.937$, $p = 0.008$; HPC: $F_{1,16} = 5.889$, $p = 0.023$) (Fig. 5C,D). These theta and beta decreases are consistent with 5-HT_{1A}R activation with DPAT, likely reflecting the serotonergic nature of RIS. In terms of PFC-HPC connectivity, RIS modestly increased delta ($F_{1,15} = 6.642$, $p = 0.017$) and decreased theta ($F_{2,20} = 5.196$, $p = 0.015$) PFC-HPC phase synchronization (Fig. 5E).

Because of its relevance as a highly prescribed drug and its serotonergic and dopaminergic nature, we aimed to gain deeper insight into the neural substrates generating RIS network effects. We first compared the

spectral profile of RIS during episodes of low locomotion following its administration (i.e. sedation) with episodes of immobility that occurred during quiet wakefulness and natural slow-wave sleep in risperidone-free sessions of one mouse where all conditions or “brain states” were tested. During risperidone-induced sedation, locomotor activity was more suppressed than during quiet wakefulness and sleep (Student’s paired t test, $p < 0.00005$) (Fig. 5F, inset). Spectral profiles were also largely distinct among brain states, especially in PFC where the power of slow waves at low frequencies (< 10 Hz) was larger than during quiet wakefulness and sedation (SWS vs. quiet rest, $p = 0.04$; SWS vs. RIS, $p = 0.006$) (Fig. 5F; also compare spectral profiles of wakefulness and sleep in Fig. 1C and sedation by RIS in Fig. 5A). Moreover, during RIS-mediated sedation a low-power narrow 4 Hz band emerged in PFC that was also present during sedation by haloperidol. In HPC, spectral profiles were more variable and also extended to higher frequencies. DPAT and M100907 also generated the 4 Hz band in PFC, although the higher rate of locomotion of the animals indicated they were in more superficial sedative-like states (Student’s unpaired t test, [Acc] RIS, haloperidol vs. DPAT or M100907, $p = 0.002$) (Fig. 5G and Supplementary Figs. 2 and 3). The 4 Hz oscillation in prelimbic PFC correlates with respiration rhythms (Moberly et al. 2018) and may be a neurophysiological marker of sedation or lethargy.

3.5. Linear regression models dissect the partial contribution of 5-HT_{1A}R, 5-HT_{2A}R and D₂R to the actions of risperidone

To better understand the involvement of 5-HT_{1A}R, 5-HT_{2A}R and D₂R to the actions of RIS, we generated linear regression models per electrode contact correlating their individual time-varying influences on neural activity of the PFC and HPC. Specifically, four different models quantified the correlation between oscillatory signals recorded during the first hour following injection of RIS with oscillatory signals recorded during the first hour following injection of DPAT ($n = 10$ electrodes, $n = 5$ mice), M100907 ($n = 15$ and 5), haloperidol ($n = 15$ and 5) and saline ($n = 11$ and 4), that were obtained in separate experimental sessions. We note that the models captured the neural pharmacodynamics generated by the drugs during the first hour after their injection. This is different from the power changes reported above which quantified average power variations at the time of maximum drug effect (~30 minutes post-injection).

In general, the proportion of variance explained (VE) by the models suggested a larger resemblance of RIS with the 5-HT and DA agents than with saline in some frequency bands (Supplementary Fig. 4). This indicated that the models could be used to estimate the partial contribution of each receptor to the actions of RIS. However, the models included potential confounding effects resulting from changes in locomotion and animal inter-variability among groups. We calculated the proportion of partial variance explained (PVE) of each drug (Fig. 6A) and the PVE of locomotion (via Acc; Supplementary Fig. 4) that allowed us to estimate separately the contribution of the drugs and locomotion to the effects of RIS (see Supplementary information). We first examined the partial contribution of locomotion across all the models. As expected, suppression of locomotor activity accounted for some RIS-mediated oscillatory changes, although its influence was unequal for all bands. High gamma was particularly influenced by locomotion with a mean PVE of 0.66 in PFC and 0.59 in HPC (mean of all models). Low gamma (0.37, 0.47 in PFC and HPC, respectively), beta (0.37, 0.32), and theta (0.3, 0.36) were moderately affected, and delta (0.19, 0.16) was affected the least (Supplementary Fig. 4). This indicated that the contribution of 5-HT and DA agents to the actions of RIS could be better estimated at lower bands, particularly at delta, and more poorly at high gamma frequencies.

When only looking at the effects of the drugs targeting individual receptors and RIS, excluding locomotion as a confounding factor, the models estimated a distinct involvement of 5-HT_{1A}R, 5-HT_{2A}R and D₂R that were also frequency-dependent. Overall, the models suggested a larger participation of the three receptors in the HPC compared to PFC (Wilcoxon Rank test; PVE DPAT in PFC vs. HPC, $p = 0.034$; PVE M100907 in PFC vs. HPC, $p = 0.002$; PVE HAL in PFC vs. HPC, $p = 0.017$; PVE saline in PFC vs. HPC, $p = 0.57$) (Fig. 6A). Moreover, they identified 5-HT_{1A}R-like reductions of beta (DPAT vs. saline, $p = 0.025$ in PFC, $p = 0.001$ in HPC) and low gamma ($p = 0.06$ in PFC, 0.002 in HPC) and 5-HT_{1A}R-like enhancement of hippocampal delta waves ($p = 0.029$). These results from the models suggest a functional resemblance of RIS and 5-HT_{1A}R agonism, particularly in the HPC. Conversely, and in agreement with the power changes reported above, RIS-induced increases of delta power were similar to D₂R antagonism with haloperidol (haloperidol vs. saline, $p < 0.00005$ in PFC, $p = 0.002$ in HPC), while in PFC the models identified a further involvement of 5-HT_{2A}R (M100907 vs. saline; $p = 0.005$). Most notably, the effects of haloperidol and

M100907 were largely coincident with RIS at high gamma frequencies (M100907 vs. saline, $p = 0.027$ in PFC, $p = 0.02$ in HPC; haloperidol vs. saline, $p = 0.024$ in PFC, $p = 0.004$ in HPC) (Table 1).

3.6. Risperidone modulates PFC-HPC network activity combining 5-HT_{1A}R, 5-HT_{2A}R and D₂R activities

The models presented above put forward a complex mechanism of action of RIS with different involvement of the three receptors depending on brain region and frequency band. To investigate further the pharmacological mechanisms proposed by the models and gain further insight into the partial contribution of 5-HT_{1A}R, 5-HT_{2A}R and D₂R to the actions of RIS onto PFC-HPC neural networks, the following series of experiments were performed: 1) administration of RIS + WAY (n = 7 mice), where 5-HT_{1A}Rs were selectively blocked after RIS to cancel its (indirect) 5-HT_{1A}R agonistic effects; 2) RIS + DOI (n = 6 mice), where 5-HT_{2A}Rs were stimulated after RIS to cancel its 5-HT_{2A}R antagonistic effects; and 3) RIS + QUI (n = 4 mice), where D₂R were stimulated after RIS to cancel its D₂R antagonistic effects. The three “reversal” drugs were administered 30 minutes after RIS. We note that the information provided by the models and the pharmacological reversals offer distinct perspectives on the issue: the models identify similarities between pharmacological activities relevant to antipsychotic drug action (i.e., RIS and the receptor activities go on the same direction), whereas the pharmacological reversals explore the rescuing abilities of agents that partly block RIS’s antipsychotic activity (i.e., RIS and the receptor activities go on the opposite direction).

None of the treatments alone could rescue RIS-induced sedation, as locomotor activity remained as low as after RIS administration (two-way mixed ANOVA with time as within factor and treatment [saline vs. RIS-WAY, saline vs. RIS-DOI, saline vs. RIS-QUI] as between factor) (Fig. 7A). Likewise, reduced MUA and theta oscillations after RIS continued at low levels after administration of WAY, DOI and quinpirole (Fig. 7B,C). However, unique effects were observed on the power of other neural oscillations. It is important to consider that WAY and DOI had little effects on oscillatory power when administered alone, whereas quinpirole produced strong changes of power that could influence the pharmacological reversal of RIS. WAY normalized RIS-induced alterations of delta and beta power in PFC and HPC and partly rescued low

gamma reductions in PFC. DOI, on the other hand, reversed RIS-mediated decreases of beta and gamma oscillations in both areas and normalized delta increases in PFC. Conversely, quinpirole accentuated the effects of RIS on beta and gamma oscillations, mimicking its effects when administered alone, but reversed RIS-induced increases of delta oscillations in both regions (Fig. 7C). This occurred despite the fact that quinpirole enlarged delta power in HPC when injected alone (Fig. 4D). We therefore postulate that D₂R contribute to RIS actions at delta but not higher frequencies (Table 2).

3.7. Proposed contribution of 5-HT_{1A}R, 5-HT_{2A}R and D₂R to the actions of RIS on PFC-HPC networks

These experiments provide evidence that 5-HT_{1A}R, 5-HT_{2A}R and D₂R contribute to RIS effects on specific neural oscillations in the PFC and HPC. RIS may act on 5-HT_{1A}R to change delta and beta oscillations and on 5-HT_{2A}R to modulate gamma oscillations. Conversely, D₂Rs participate in the generation of RIS-induced delta oscillations. Intriguingly, quinpirole exacerbated RIS effects further on beta and gamma oscillations. Therefore, a contribution of D₂R to RIS-mediated changes in these higher-frequency oscillations is plausible.

4. Discussion

The main objective of this study was to establish the neural mechanisms of RIS in respect to its serotonergic and dopaminergic properties in a brain circuit crucial for cognitive processing and severely impaired in schizophrenia. Typical and atypical APDs haloperidol and RIS block D₂R with high affinity, while RIS also blocks 5-HT_{2A}R and stimulates 5-HT_{1A}R indirectly (Meltzer and Massey, 2011). Here we demonstrate that 5-HT_{1A}R agonism, 5-HT_{2A}R/D₂R antagonism and RIS exert strong inhibitory actions on neural network activity of the PFC-HPC circuit in freely-moving mice. Moreover, pharmacological reversal experiments helped elucidate the complex neural mechanisms of action of RIS, specifically clarifying the contributions of 5-HT_{1A}R, 5-HT_{2A}R and D₂R in the PFC-HPC circuit, which are further emphasized by statistical modeling of associations between time-varying power activities.

APDs caused deeper lethargy than serotonergic agents that act only on one receptor, as reflected by their greater suppression of locomotion. The cellular mechanisms for APD-induced sedation have been associated

with 5-HT_{2A}R antagonism (Joshi et al., 2017; Williams et al., 2012). Consistently, M100907 produced sedation-like effects in this study. DPAT also caused moderate sedation, suggesting the potential involvement of 5-HT_{1A}R as well (Misslin et al., 1990). Furthermore, a participation of D₂R in sedation is also plausible due to the high affinity of haloperidol for these receptors and its marked sedative effects. The mechanisms for APD-sedation have also been attributed to histamine H₁R (Miller, 2004), for which RIS has moderate affinity. Therefore, RIS-induced sedation may result from the cooperation of 5-HT_{1A}R indirect agonism and 5-HT_{2A}R/D₂R antagonism and H₁R. Sedation correlated with a general depression of neural spiking, theta and gamma oscillations in PFC and HPC, and a narrow 4 Hz band in PFC. A 4 Hz oscillation has been reported in the prelimbic PFC of mice during fear behaviors (freezing) that may be generated by respiration rhythms (Karalis et al., 2016; Moberly et al., 2018). So here this band may be particularly visible due to strong respiration and marked theta power attenuation induced by the drugs. Our findings on the neural substrates of sedation are consistent with human studies demonstrating distinct oscillatory profiles of anesthetics causing sedation and slow-wave sleep (Akeju and Brown, 2017). As mentioned above, the three receptors under investigation (plus H₁R) may cooperate to cause sedation by RIS. This agrees with the fact that manipulation of individual receptors after RIS administration in reversal experiments was not sufficient to rescue sedation, and thus locomotor activity, MUA and theta oscillations remained at RIS-induced low levels. Gamma oscillations were the exception, as they were largely reversed by 5-HT_{2A}R activation after RIS. This may be due to the selective enhancement of gamma oscillations caused by DOI (see below). Changes in MUA and gamma oscillations are inextricably tied (Buzsáki and Wang, 2012), so a drug-induced decrease of MUA may inevitably attenuate gamma rhythms. The APD-mediated gamma reductions agree with previous studies showing that acute APDs normalize excessive gamma power in the EEG of both schizophrenia patients (Uhlhaas and Singer, 2010) and rodent models of schizophrenia (Ahnaou et al., 2017; Jones et al., 2012). In addition, the two APDs mimicked the hippocampal theta-power reductions produced by DPAT and M100907. Hippocampal theta waves are strongly associated with locomotion (Buzsáki, 2002), so their drug-induced weakening may also contribute to animals' immobility.

Our study demonstrates that 5-HT_{1A}R agonism and 5-HT_{2A}R/D₂R antagonism disrupt PFC and HPC theta, gamma oscillations and PFC-HPC theta synchrony, suggesting that these pharmacological activities may

directly mediate theta and gamma attenuation by many APDs. Prefronto-hippocampal theta and gamma oscillations and theta synchronization play relevant roles in cognitive processing (Benchenane et al., 2011; Fries, 2009) and therefore their disruption by 5-HT_{1A}R agonism and 5-HT_{2A}R/D₂R antagonism should be detrimental for cognitive processing in healthy mice. Furthermore, PFC-HPC theta-gamma connectivity is abnormal in patients with schizophrenia and related animal models (Sigurdsson et al., 2010; Spencer et al., 2003; Uhlhaas and Singer, 2010). However, 5-HT_{1A}R agonism and 5-HT_{2A}R antagonism can ameliorate executive function in phencyclidine-treated mice (Oyamada et al., 2015), an established mouse model of schizophrenia. We note that in this study drug effects were investigated in healthy mice, however in order to properly characterize PFC-HPC circuitry in schizophrenia it is necessary to understand how APDs, serotonin and dopamine receptors affect a normal PFC-HPC circuit.

In addition, 5-HT_{2A}R/D₂R antagonism and RIS markedly increased delta oscillations in the PFC and HPC. Delta oscillations play a role during sleep, but their contribution to brain function during alertness and cognitive processing is unclear. They emerge in frontal areas when subjects need to inhibit a motor response or ignore distracting sensory information and, in agreement, they are prominent during meditation. Thus, delta waves are likely inhibitory oscillations that prevent the activity of subcortical networks that should remain inactive during the execution of a task (Harmony, 2013). The consequences of increased delta oscillations after RIS are unclear but we speculate they may have been associated with RIS-induced sedation. On a different note, 5-HT_{1A}R agonism and RIS decreased beta oscillations in PFC and HPC. Beta oscillations are involved in decision making (Haegens et al., 2017) and, interestingly, they are increased in schizophrenia patients that suffer from auditory hallucinations (Lee et al., 2006).

5-HT_{1A}R activation greatly reduced neural activity of prefronto-hippocampal networks in agreement with its inhibitory effects on postsynaptic transmission. Similarly, 5-HT_{2A}R blockade prevented 5-HT_{2A}R-mediated excitability also disrupting neural network activity (Celada et al., 2013). On the contrary, activation of 5-HT_{2A}R with DOI specifically increased high gamma oscillations in PFC and PFC-HPC high gamma connectivity, having little effects on other oscillatory activities, locomotion or MUA. DOI is a 5-HT_{2A/2C}R agonist, but the high gamma increase was blocked by M100907, implicating 5-HT_{2A}R in their generation. These results suggest that DOI's hallucinogenic effects may originate from selective enhancement of

prefrontal high gamma oscillations that travel to subcortical structures, as indicated by increased PFC-HPC connectivity at the same frequency. 5-HT_{2A}R antagonism exerted strong inhibitory effects when administered alone that were more pronounced after administration of DOI, as reflected by larger z-score variations. So, the therapeutic actions of pharmacologically blocking 5-HT_{2A}R may be more efficient under psychotomimetic scenarios. The high gamma increase by DOI in conjunction with the high gamma decrease by DPAT supports the notion that 5-HT_{1A}R and 5-HT_{2A}R play complementary roles in regulating PFC high-gamma oscillations via 5-HT_{1A}R- and 5-HT_{2A}R-expressing fast-spiking interneurons, as suggested by our previous work in rats (Puig et al., 2010). 5-HT_{2A}R agonists such as DOI and lysergic acid diethylamine (LSD) produce hallucinations in human subjects that correlate with increases of PFC metabolism (Nichols, 2004) and, in fact, hallucinogens acting at 5-HT_{1A/2A}R such as 5MeO-DMT increase PFC gamma oscillations (Riga et al., 2017). Therefore, excessive PFC high-gamma oscillations may underlie the psychotomimetic actions of DOI. We extend this by proposing that this amplified cortical gamma transmission projects to subcortical structures via PFC-HPC high gamma connectivity. Quinpirole, that causes psychotomimetic effects in rodents like DOI (Asaoka et al., 2019), produced moderate increases of PFC low gamma power. However, this was not accompanied by an elevated PFC-HPC gamma functional connectivity.

We further aimed to characterize the contribution of 5-HT_{1A}R, 5-HT_{2A}R and D₂R to the actions of RIS on PFC-HPC networks via linear regression modeling and pharmacological reversal. In an effort to disentangle the observed changes in neural activity from the immobility caused by the drugs, we developed models that took locomotion into account allowing a better estimation of the genuine similarities between the actions produced by the three receptors and RIS on neural activity at short timescales (1 minute). Reduction in animals' movement was highly associated with high-gamma-band attenuation in both areas. However, we note that the models still identified significant differences between M100907/haloperidol and saline in the two brain structures. Consistent with the results obtained from the average power changes, the models identified a match between the time-varying actions of RIS and DPAT in several frequency bands (delta, beta and low gamma), that was different from the similarity between RIS and M100907 (delta and high gamma) and RIS and quinpirole (delta, low and high gamma). Therefore, each of the receptors, alone or in combination, could participate in RIS-induced effects depending on the frequency band. Pharmacological

reversals after RIS supported these results. Both the power changes and pharmacological reversal of RIS revealed that both activation and inhibition of D₂R exert similar effects on PFC-HPC activity. We therefore conclude that a fine range of D₂R activation is necessary for correct neural network function. This provides further support for a U-shaped function describing how D₂R modulate brain activity (Horst et al., 2019; Puig and Miller, 2015).

The results outlined in this study suggest an important role of 5-HT_{1A}R in the action of RIS despite the lower affinity of RIS for 5-HT_{1A}R in comparison with 5-HT_{2A}R and D₂R. This implies that 5-HT_{1A}R-mediated network effects of RIS arise from pharmacological interactions of the serotonin and dopamine systems. This is supported by studies that show that 5-HT_{1A}R, but not 5-HT_{2A}R, are necessary for RIS and other APDs to elevate PFC dopamine *in vivo* (Bortolozzi et al., 2010; Ichikawa et al., 2001). The ability of many APDs to improve negative and cognitive symptoms in schizophrenia has been attributed to their capacity to increase dopamine-mediated transmission in PFC and HPC, and optimal dopamine transmission is critical for normal cognitive processing (Puig et al., 2014; Puig and Miller, 2012, 2015). In addition, 5-HT_{1A}R and 5-HT_{2A}R are largely co-expressed in pyramidal neurons of the PFC where they interact functionally (Amargós-Bosch et al., 2004).

The dose of RIS used in this study may have been slightly high as it caused deep sedation of mice. However, two aspects of our results suggest that our findings are relevant for the understanding of the effects of RIS on PFC-HPC circuits. First, RIS-induced effects could be partly or fully reversed by WAY, DOI and quinpirole at several frequency bands. And second, the statistical models identified significant similarities between RIS and the effects of WAY, DOI and quinpirole even when the contribution of locomotion was minimized. In fact, a recent study has reported that acute RIS injected at 1 mg/kg, but not at lower doses, is effective in rescuing memory impairments in mice treated with phencyclidine, a pharmacological model of schizophrenia (Adem et al., 2019). Another limitation of this study is that RIS was administered acutely. However it is typically prescribed chronically to schizophrenia patients. Moreover, APDs almost certainly act on dopamine receptors of the striatum and other brain regions. Further studies will have to determine how 5-HT_{1A}R agonism, 5-HT_{2A}R/D₂R antagonism and chronic administration of APDs affect theta, gamma oscillations and theta connectivity in cortico-hippocampal and cortico-striatal circuits under psychotomimetic scenarios.

In summary, this study characterizes how 5-HT_{1A}R, 5-HT_{2A}R, D₂R and RIS influence PFC-HPC neural network activity and provides novel insight into the neural mechanisms of widely used psychiatric medication including APDs.

Acknowledgements

We would like to thank Drs. F. Artigas, R. de la Torre and P. Robledo and Ms. A. Fath for helpful comments on this manuscript. Author contributions: TG, ATC, MAG and MVP designed research; TG, MAG, CDS and PN performed research; TG, ATC, MAG, PN, CDS, JC and MVP analyzed data; TG, ATC, MAG and MVP wrote the paper. The authors declare no conflict of interest. This work was supported by the Brain and Behavior Research Foundation (NARSAD Young Investigator Award 23014), SAF2013-49129-C2-2-R and SAF2016-80726-R (AEI/FEDER, UE) by the Spanish Ministry of Economy and Competitiveness (MINECO; to MVP). M.V. Puig is a Ramon y Cajal Investigator (RyC-2012-10042), M. Alemany a FPI predoctoral fellow (BES-2014-070429) from MINECO, and C. Delgado a FI predoctoral fellow (2018 FI_B_00112) from the Generalitat de Catalunya (AGAUR).

References

- Adem, A., Madjid, N., Stiedl, O., Bonito-Oliva, A., Konradsson-Geuken, Å., Holst, S., Fisone, G., Ögren, S.O., 2019. Atypical but not typical antipsychotic drugs ameliorate phencyclidine-induced emotional memory impairments in mice. *Eur. Neuropsychopharmacol.* 29, 616–628.
- Ahnaou, A., Huysmans, H., Van de Castele, T., Drinkenburg, W.H.I.M., 2017. Cortical high gamma network oscillations and connectivity: a translational index for antipsychotics to normalize aberrant neurophysiological activity. *Transl. Psychiatry* 7, 1285.
- Akeju, O., Brown, E.N., 2017. Neural oscillations demonstrate that general anesthesia and sedative states are neurophysiologically distinct from sleep. *Curr. Opin. Neurobiol.* 44, 178–185.
- Amargós-Bosch, M., Bortolozzi, A., Puig, M.V., Serrats, J., Adell, A., Celada, P., Toth, M., Mengod, G., Artigas, F., 2004. Co-expression and in vivo interaction of serotonin1A and serotonin2A receptors in pyramidal neurons of prefrontal cortex. *Cereb. Cortex* 14, 281–299.
- Asaoka, N., Nishitani, N., Kinoshita, H., Nagai, Y., Hatakama, H., Nagayasu, K., Shirakawa, H., Nakagawa, T., Kaneko, S., 2019. An adenosine A_{2A} receptor antagonist improves multiple symptoms of repeated quinpirole-induced psychosis. *eneuro* 6, ENEURO.0366-18.2019.
- Benchenane, K., Tiesinga, P.H., Battaglia, F.P., 2011. Oscillations in the prefrontal cortex: a gateway to memory and attention. *Curr. Opin. Neurobiol.* 21, 475–485.
- Berumen, L.C., Rodríguez, A., Mileli, R., García-Alcocer, G., 2012. Serotonin receptors in hippocampus. *Sci. World J.* 2012.
- Bokil, H., Andrews, P., Kulkarni, J.E., Mehta, S., Mitra, P.P., 2010. Chronux: a platform for analyzing neural signals. *J. Neurosci. Methods* 192, 146–51.
- Bortolozzi, A., Castañé, A., Semakova, J., Santana, N., Alvarado, G., Cortés, R., Ferrés-Coy, A., Fernández, G., Carmona, M.C., Toth, M., Perales, J.C., Monteféltro, A., Artigas, F., 2012. Selective siRNA-mediated suppression of 5-HT_{1A} autoreceptors evokes strong anti-depressant-like effects. *Mol. Psychiatry* 17, 612–623.
- Bortolozzi, A., Masana, M., Díaz-Mataix, L., Cortés, R., Scorza, M.C., Gingrich, J.A., Toth, M., Artigas, F., 2010. Dopamine release induced by atypical antipsychotics in prefrontal cortex requires 5-HT_{1A} receptors but not 5-HT_{2A} receptors. *Int. J. Neuropsychopharmacol.* 13, 1299–1314.
- Brookshire, B.R., Jones, S.R., 2009. Direct and indirect 5-HT receptor agonists produce gender-specific effects on locomotor and vertical activities in C57 BL/6J mice. *Pharmacol. Biochem. Behav.* 94, 194–203.
- Buzsáki, G., 2002. Theta oscillations in the hippocampus. *Neuron* 33, 325–340.
- Buzsáki, G., Wang, X.-J., 2012. Mechanisms of gamma oscillations. *Annu. Rev. Neurosci.* 35, 203–25.
- Celada, P., Puig, M.V., Artigas, F., 2013. Serotonin modulation of cortical neurons and networks. *Front. Integr. Neurosci.* 7, 25.
- Egashira, N., Koushi, E., Mishima, K., Iwasaki, K., Oishi, R., Fujiwara, M., 2007. 2,5-Dimethoxy-4-iodoamphetamine (DOI) inhibits Delta9-tetrahydrocannabinol-induced catalepsy-like immobilization in mice. *J. Pharmacol. Sci.* 105, 361–6.
- Fries, P., 2009. Neuronal gamma-band synchronization as a fundamental process in cortical computation. *Annu. Rev. Neurosci.* 32, 209–224.
- Gallitano-Mendel, A., Wozniak, D.F., Pehek, E.A., Milbrandt, J., 2008. Mice lacking the immediate early

gene *Egr3* respond to the anti-aggressive effects of clozapine yet are relatively resistant to its sedating effects. *Neuropsychopharmacology* 33, 1266–1275.

- Gee, S., Ellwood, I., Patel, T., Luongo, F., Deisseroth, K., Sohal, V.S., 2012. Synaptic activity unmasks dopamine D2 receptor modulation of a specific class of layer V pyramidal neurons in prefrontal cortex. *J. Neurosci.* 32, 4959–4971.
- Groenewegen, H.J., Uylings, H.B., 2000. The prefrontal cortex and the integration of sensory, limbic and autonomic information. *Prog. Brain Res.* 126, 3–28.
- Haegens, S., Vergara, J., Rossi-Pool, R., Lemus, L., Romo, R., 2017. Beta oscillations reflect supramodal information during perceptual judgment. *Proc. Natl. Acad. Sci. USA* 114, 13810–13815.
- Hardmeier, M., Hatz, F., Bousleiman, H., Schindler, C., Stam, C.J., Fuhr, P., 2014. Reproducibility of functional connectivity and graph measures based on the phase lag index (PLI) and weighted phase lag index (wPLI) derived from high resolution EEG. *PLoS One* 9, e108648.
- Harmony, T., 2013. The functional significance of delta oscillations in cognitive processing. *Front. Integr. Neurosci.* 7:83.
- Heckers, S., Konradi, C., 2010. Hippocampal pathology in schizophrenia, in: Swerdlow, N.R. (Ed.), *Behavioral Neurobiology of Schizophrenia and Its Treatment*. Heidelberg: Springer, pp. 529–553.
- Hensler, J.G., 2006. Serotonergic modulation of the limbic system. *Neurosci. Biobehav. Rev.* 30, 203–214.
- Horst, N.K., Jupp, B., Roberts, A.C., Robbins, T.W., 2019. D2 receptors and cognitive flexibility in marmosets: tri-phasic dose-response effects of intra-striatal quinpirole on serial reversal performance. *Neuropsychopharmacology* 44, 564–571.
- Ichikawa, J., Ishii, H., Bonaccorso, S., Fowler, W.L., O’Laughlin, I.A., Meltzer, H.Y., 2001. 5-HT_{2A} and D2 receptor blockade increases cortical DA release via 5-HT_{1A} receptor activation: a possible mechanism of atypical antipsychotic-induced cortical dopamine release. *J. Neurochem.* 76, 1521–1531.
- Jones, N.C., Reddy, M., Anderson, P., Salzberg, M.R., O’Brien, T.J., Pinault, D., 2012. Acute administration of typical and atypical antipsychotics reduces EEG γ power, but only the preclinical compound LY379268 reduces the ketamine-induced rise in γ power. *Int. J. Neuropsychopharmacol.* 15, 657–68.
- Joshi, R.S., Quadros, R., Drumm, M., Ain, R., Panicker, M.M., 2017. Sedative effect of Clozapine is a function of 5-HT_{2A} and environmental novelty. *Eur. Neuropsychopharmacol.* 27, 70–81.
- Karalis, N., Dejean, C., Chaudun, F., Khoder, S., Rozeske, R.R., Wurtz, H., Bagur, S., Benchenane, K., Sirota, A., Courtin, J., Herry, C., 2016. 4-Hz oscillations synchronize prefrontal-amygdala circuits during fear behavior. *Nat. Neurosci.* 19, 605–12.
- Kocsis, B., Varga, V., Dahan, L., Sik, A., 2006. Serotonergic neuron diversity: Identification of raphe neurons with discharges time-locked to the hippocampal theta rhythm. *Proc. Natl. Acad. Sci. U. S. A.* 103, 1059–1064.
- Lavin, A., Nogueira, L., Lapish, C.C., Wightman, R.M., Phillips, P.E.M., Seamans, J.K., 2005. Mesocortical dopamine neurons operate in distinct temporal domains using multimodal signaling. *J. Neurosci.* 25, 5013–5023.
- Lee, S.H., Wynn, J.K., Green, M.F., Kim, H., Lee, K.J., Nam, M., Park, J.K., Chung, Y.C., 2006. Quantitative EEG and low resolution electromagnetic tomography (LORETA) imaging of patients with persistent auditory hallucinations. *Schizophr. Res.* 83, 111–9.
- Mattia, M., Ferraina, S., Del Giudice, P., 2010. Dissociated multi-unit activity and local field potentials: A theory inspired analysis of a motor decision task. *Neuroimage* 52, 812–823.

- Meltzer, H., Massey, B., 2011. The role of serotonin receptors in the action of atypical antipsychotic drugs. *Curr. Opin. Pharmacol., Neurosciences* 11, 59–67.
- Meltzer, H.Y., Huang, M., 2008. In vivo actions of atypical antipsychotic drug on serotonergic and dopaminergic systems, in: *Serotonin and Dopamine Interaction: Experimental Evidence and Therapeutic Relevance*. Elsevier, pp. 177–197. 6
- Meltzer, H.Y., W. Massey, B., Horiguchi, M., 2012. Serotonin receptors as targets for drugs useful to treat psychosis and cognitive impairment in schizophrenia. *Curr. Pharm. Biotechnol.* 13, 1572–1586.
- Miller, D.D., 2004. Atypical antipsychotics: sleep, sedation, and efficacy. *Prim. Care Companion J. Clin. Psychiatry* 6, 3–7.
- Minzenberg, M.J., Laird, A.R., Thelen, S., Carter, C.S., Glahn, D.C., 2009. Meta-analysis of 41 functional neuroimaging studies of executive function in schizophrenia. *Arch. Gen. Psychiatry* 66, 811.
- Misslin, R., Griebel, G., Saffroy-Spittler, M., Vogel, E., 1990. Anxiolytic and sedative effects of 5-HT_{1A} ligands, 8-OH-DPAT and MDL 73005EF, in mice. *Neuroreport* 1, 267–70.
- Moberly, A.H., Schreck, M., Bhattarai, J.P., Zweifel, L.S., Luo, W., Ma, M., 2018. Olfactory inputs modulate respiration-related rhythmic activity in the prefrontal cortex and freezing behavior. *Nat. Commun.* 9, 1528.
- Nichols, D.E., 2004. Hallucinogens. *Pharmacol. Ther.* 101, 131–181.
- Oyamada, Y., Horiguchi, M., Rajagopal, L., Miyauchi, M., Meltzer, H.Y., 2015. Combined serotonin (5-HT)_{1A} agonism, 5-HT_{2A} and dopamine D₂ receptor antagonism reproduces atypical antipsychotic drug effects on phencyclidine-impaired novel object recognition in rats. *Behav. Brain Res., SI: Object Recognition Memory in Rats and Mice* 285, 165–175.
- Puig, M.V., Antzoulatos, E.G., Miller, E.K., 2014. Prefrontal dopamine in associative learning and memory. *Neuroscience* 282.
- Puig, M.V., Miller, E.K., 2015. Neural substrates of dopamine d₂ receptor modulated executive functions in the monkey prefrontal Cortex. *Cereb. Cortex* 25, 2980–2987.
- Puig, M.V., Miller, E.K., 2012. The role of prefrontal dopamine D₁ receptors in the neural mechanisms of associative learning. *Neuron* 74, 874–886.
- Puig, M.V., Watakabe, A., Ushimaru, M., Yamamori, T., Kawaguchi, Y., 2010. Serotonin modulates fast-spiking interneuron and synchronous activity in the rat prefrontal cortex through 5-HT_{1A} and 5-HT_{2A} receptors. *J. Neurosci.* 30, 2211–2222.
- Puighermanal, E., Biever, A., Espallergues, J., Gangarossa, G., De Bundel, D., Valjent, E., 2015. *drd2-cre:ribotag* mouse line unravels the possible diversity of dopamine d₂ receptor-expressing cells of the dorsal mouse hippocampus. *Hippocampus* 25, 858–875.
- Riga, M.S., Lladó-Pelfort, L., Artigas, F., Celada, P., 2017. The serotonin hallucinogen 5-MeO-DMT alters cortico-thalamic activity in freely moving mice: Regionally-selective involvement of 5-HT_{1A} and 5-HT_{2A} receptors. *Neuropharmacology* 219–230.
- Roth, B., Hanizavareh, S.M., Blum, A., 2004. Serotonin receptors represent highly favorable molecular targets for cognitive enhancement in schizophrenia and other disorders. *Psychopharmacology (Berl)*. 174, 17–24.
- Santana, N., Mengod, G., Artigas, F., 2009. Quantitative analysis of the expression of dopamine D₁ and D₂ receptors in pyramidal and GABAergic neurons of the rat prefrontal cortex. *Cereb. Cortex* 19, 849–860.

- Schmid, C.L., Raehal, K.M., Bohn, L.M., 2008. Agonist-directed signaling of the serotonin 2A receptor depends on beta-arrestin-2 interactions in vivo. *Proc. Natl. Acad. Sci. U. S. A.* 105, 1079–84.
- Sigurdsson, T., Duvarci, S., 2016. Hippocampal-prefrontal interactions in cognition, behavior and psychiatric disease. *Front. Syst. Neurosci.* 9, 190.
- Sigurdsson, T., Stark, K.L., Karayiorgou, M., Gogos, J.A., Gordon, J.A., 2010. Impaired hippocampal–prefrontal synchrony in a genetic mouse model of schizophrenia. *Nature* 464, 763–767.
- Spencer, K.M., Nestor, P.G., Niznikiewicz, M.A., Salisbury, D.F., Shenton, M.E., McCarley, R.W., 2003. Abnormal neural synchrony in schizophrenia. *J. Neurosci.* 23, 7407–7411.
- Stam, C.J., Nolte, G., Daffertshofer, A., 2007. Phase lag index: assessment of functional connectivity from multi channel EEG and MEG with diminished bias from common sources. *Hum. Brain Mapp.* 28, 1178–93.
- Stark, E., Abeles, M., 2007. Predicting movement from multiunit activity. *J. Neurosci.* 27, 8387–8394.
- Uhlhaas, P.J., Singer, W., 2010. Abnormal neural oscillations and synchrony in schizophrenia. *Nat. Rev. Neurosci.* 11, 100–113.
- Vertes, R.P., Kinney, G.G., Kocsis, B., Fortin, W.J., 1994. Pharmacological suppression of the median raphe nucleus with serotonin1a agonists, 8-OH-DPAT and buspirone, produces hippocampal theta rhythm in the rat. *Neuroscience* 60, 441–451.
- Vinck, M., Oostenveld, R., Van Wingerden, M., Battaglia, F., Pennartz, M.A., 2011. An improved index of phase-synchronization for electrophysiological data in the presence of volume-conduction, noise and sample-size bias. *Neuroimage* 55, 1548-1565.
- Wang, S., Che, T., Levit, A., Shoichet, B.K., Wacker, D., Roth, B.L., 2018. Structure of the D2 dopamine receptor bound to the atypical antipsychotic drug risperidone. *Nature* 555, 269–273.
- Williams, A.A., Ingram, W.M., Levine, S., Resnik, J., Kamel, C.M., Lish, J.R., Elizalde, D.I., Janowski, S.A., Shoker, J., Kozlenkov, A., González-Maeso, J., Gallitano, A.L., 2012. Reduced levels of serotonin 2A receptors underlie resistance of Egr3-deficient mice to locomotor suppression by clozapine. *Neuropsychopharmacology* 37, 2285–98.
- Wu, L., Feng, X., Li, T., Sun, B., Khan, M.Z., He, L., 2017. Risperidone ameliorated A β 1-42 -induced cognitive and hippocampal synaptic impairments in mice. *Behav. Brain Res.* 322, 145–156.

Table 1. Summary of main changes per brain area and frequency band

Drug	Activity	4 Hz Band*		Delta (3-5 Hz)		Theta (8-10 Hz)		Beta (15-25 Hz)		Low Gamma (30-50 Hz)		High Gamma (51-100 Hz)		MUA	
		PFC	HPC	PFC	HPC	PFC	HPC	PFC	HPC	PFC	HPC	PFC	HPC	PFC	HPC
DPAT	<i>1A agonist</i>	↑	-	-	-	↓	↓	↓	↓	↓	↓	↓	↓	↓	↓
WAY	<i>1A antago.</i>	-	-	-	-	-	-	-	↑	-	-	↓	-	↓	-
DOI	<i>2A agonist</i>	-	-	-	-	-	-	-	-	-	-	↑	-	↓	-
M100	<i>2A antago.</i>	↑	-	↑	↑	↓	↓	-	-	↓	↓	↓	↓	↓	↓
QUI	<i>D2 agonist</i>	-	-	-	↑	↓	↓	↓	↓	-	-	↓	↓	↓	↓
HAL	<i>D2 antago.</i>	↑	-	↑	↑	-	↓	-	-	↓	↓	↓	↓	↓	↓
	<i>Typic. APD</i>	↑	-	↑	↑	-	↓	-	-	↓	↓	↓	↓	↓	↓
RIS	<i>Atypical APD</i>	↑	-	↑	↑	↓	↓	↓	↓	↓	-	↓	↓	↓	↓

Summary of main power changes per brain area and frequency band (minutes 25-35 after drug injections). MUA changes are also included. *Measured during awake immobility episodes only. It is generated during sedative or sedative-like (lethargic) states.

Table 2. Potential pharmacological activities of RIS per brain area and frequency band

Brain region	Delta (3-5 Hz)	Theta (8-10 Hz)	Beta (15-25 Hz)	Low Gamma (30-50 Hz)	High Gamma (51-100 Hz)
PFC	1A, 2A, D2	-	1A, 2A	1A, 2A	2A
HPC	1A, D2	-	2A	2A	2A

Summary of the putative contribution of the three receptors to RIS effects revealed by pharmacological reversals. Pharmacological activities not detected by the models are highlighted in red. Distinct combinations of the receptors may underlie RIS effects depending on the frequency band, with a prominent role of 5-HT receptors over D₂R. Low gamma oscillations were the least predicted by the models so the cellular mechanisms may be particularly complex for this band.

Figures and figure legends

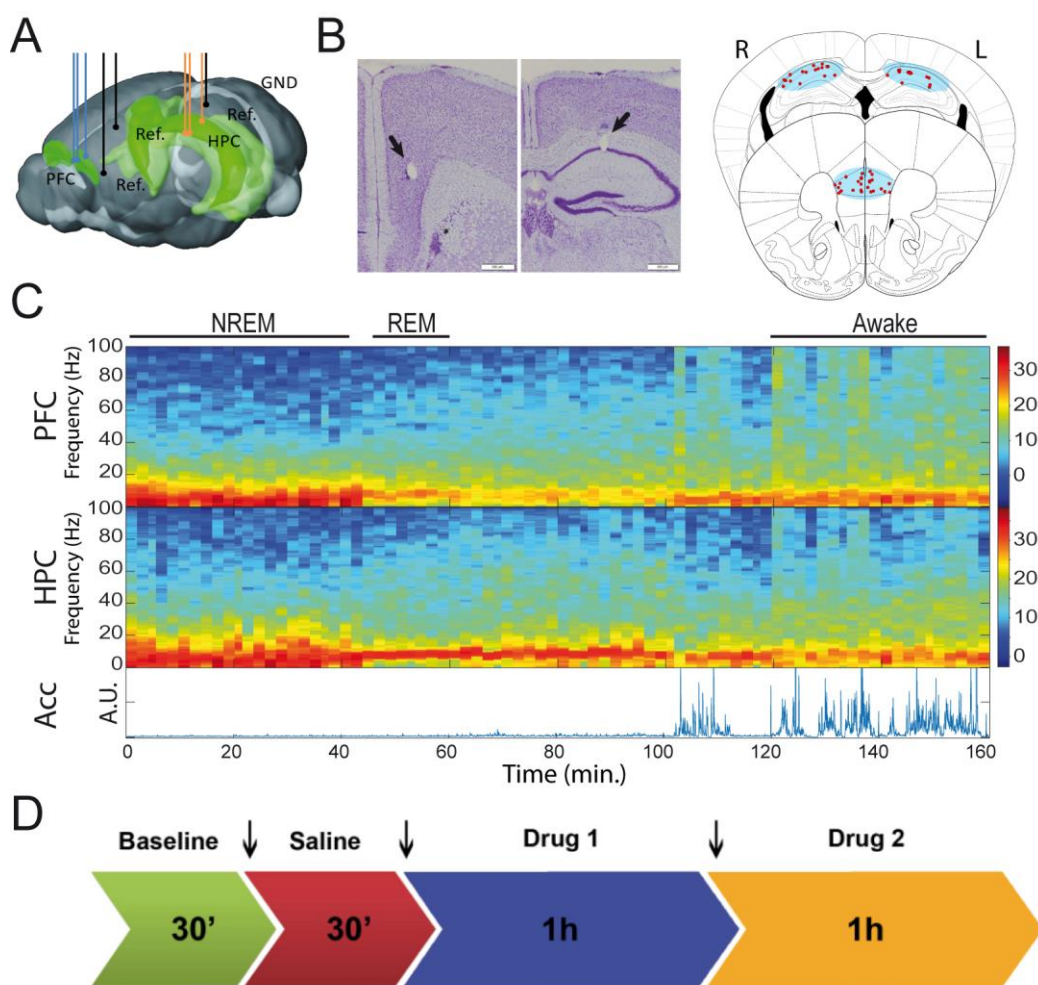


Figure 1. (A) Diagram of electrode implantation in the PFC and HPC of the mouse brain. Three electrodes were implanted in each area together with three reference electrodes used for the calculation of MUA. GND refers to the screw used as ground by the recording system. (B) Representative images of brain sections stained with Cresyl violet. Arrows denote the location of electrode tips in the prelimbic PFC (left) and the CA1 area of the HPC (right). Also shown is a schematic summary of the electrodes' locations in all the animals (right or left hemispheres). (C) Example of a neural recording in one mouse during alertness and natural sleep (NREM and REM episodes). Shown are spectrograms of neural signals in the PFC and HPC and the corresponding instantaneous variance of the acceleration (Acc) used to identify the distinct brain states (awake versus asleep; see also Supplementary Fig. 1). (D) Experimental protocol. Lines denote the 30 min episodes used for quantification of neural signals.

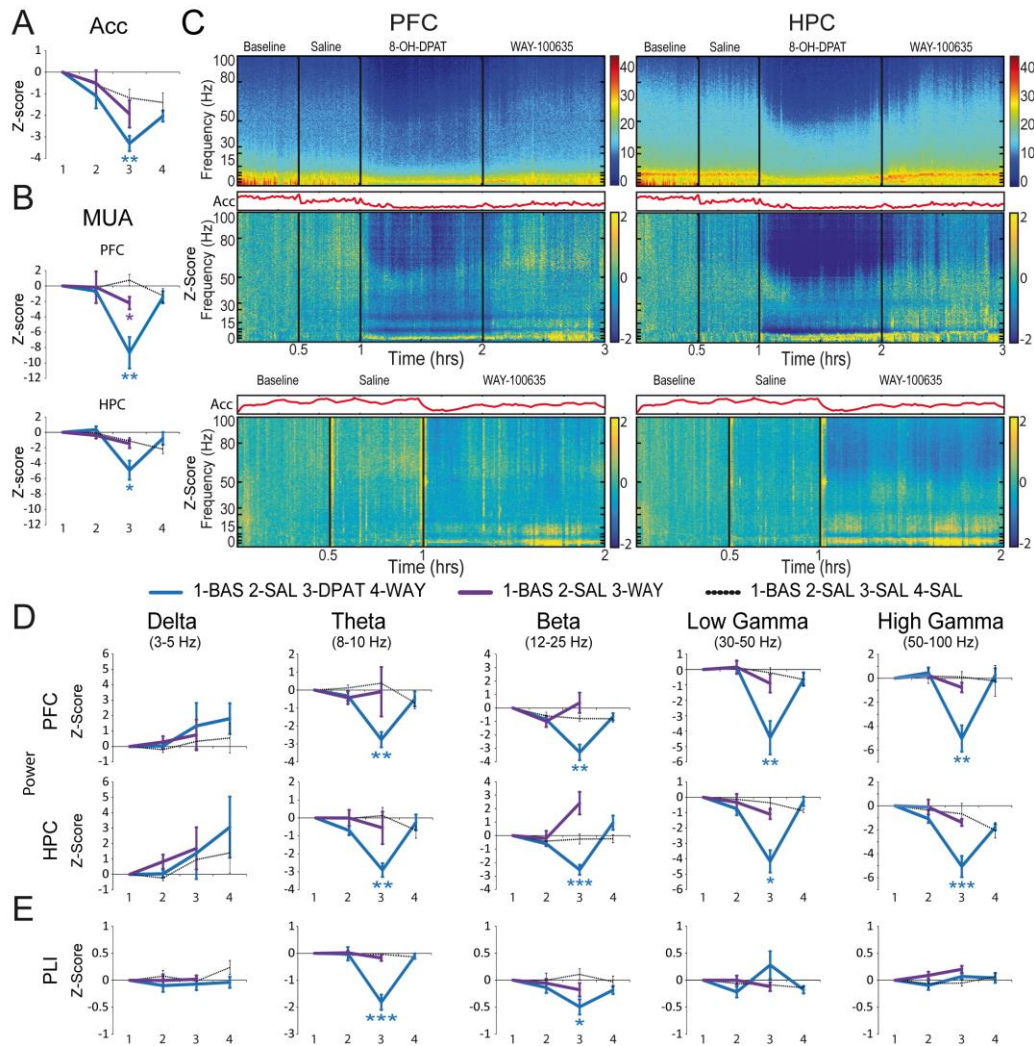


Figure 2. Selective activation of 5-HT_{1A}R with 8-OH-DPAT (DPAT; n = 8 mice) decreases locomotion, multi-unit-activity (MUA), power of theta, beta, low gamma and high gamma oscillations in PFC and HPC and PFC-HPC theta and beta phase synchronization. Selective inhibition of 5-HT_{1A}R with WAY-100635 (WAY; n = 6 mice) exerts small effects on the PFC-HPC circuit. **(A)** Group effects (z-scores relative to baseline) of changes in the variance of the accelerometer (Acc) after initial saline controls (last 10 min), DPAT (min 25-35 after DPAT injections), and reversal by WAY (min 25-35 after WAY injections). Saline only and saline-WAY groups are also shown. **(B)** Group effects (z-scores) of changes in MUA in PFC and HPC. **(C)** Individual (one electrode) examples of changes in power over time after DPAT-WAY (upper panels) and group effects for DPAT-WAY and WAY alone (lower panels). Black lines indicate time of saline, DPAT and WAY administrations. Mean Acc is also shown in red (in arbitrary units). Note the narrow 4 Hz band that emerges in the PFC after DPAT (see also Supplementary Figure 2). **(D)** Quantification of changes in power (z-scores). **(E)** Quantification of changes in phase-lag index (PLI) (z-scores). In all figures: shown are quantifications of z-score medians; colorbars reflect power z-scores with respect to baseline (zero indicates no change); error bars indicate standard error of the mean; **p* < .05, ***p* < .01, ****p* < .001 versus the saline group.

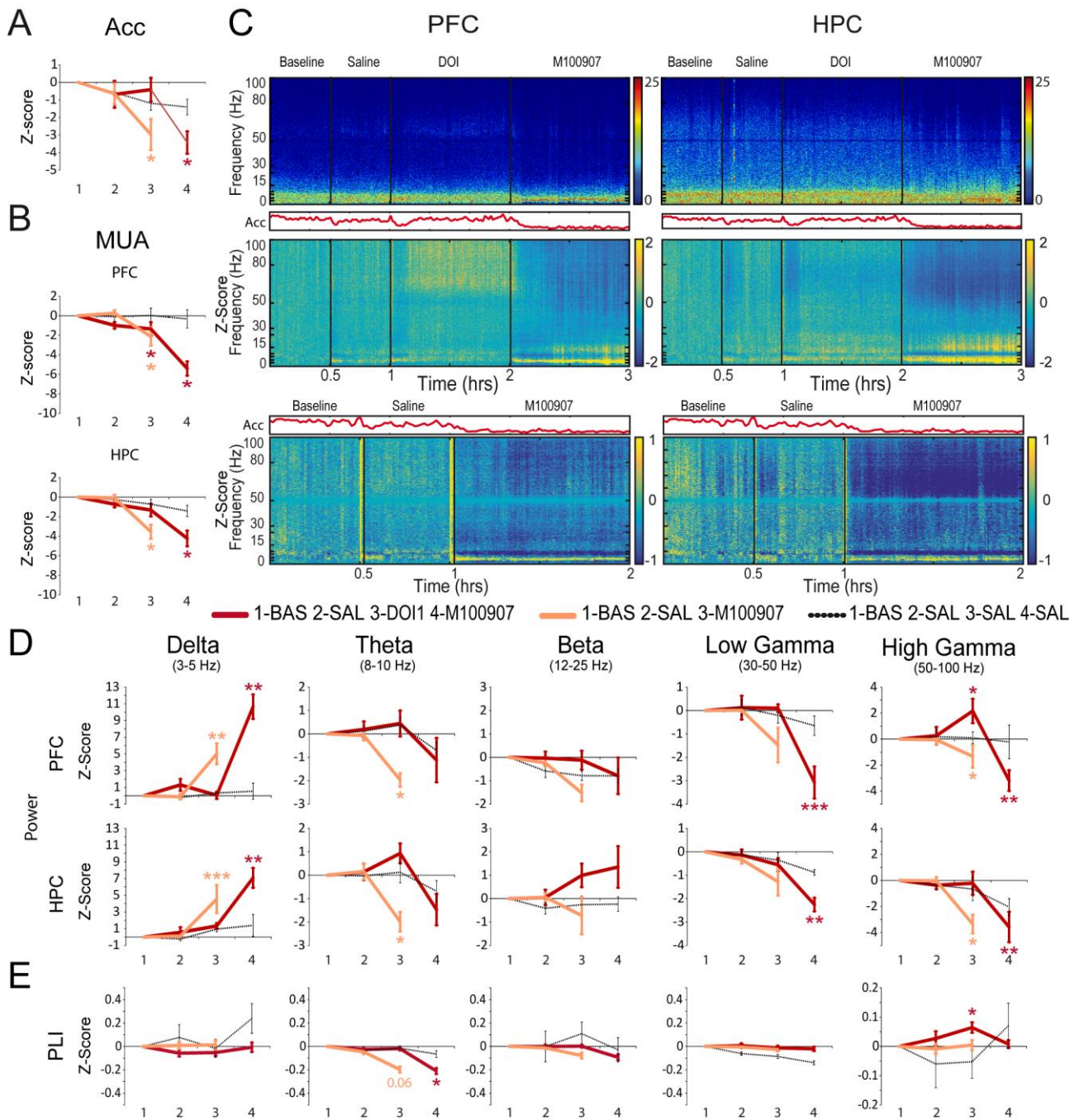


Figure 3. Activation of 5-HT_{2A}R with DOI (n = 7 mice) produces a selective enhancement of PFC high-gamma oscillations and PFC-HPC high gamma phase synchronization. Selective inhibition of 5-HT_{2A}R with M100907 (n = 8 mice) decreases locomotion, MUA, power of theta, low gamma and high gamma oscillations in PFC and HPC and PFC-HPC theta phase synchronization while increasing delta waves. **(A)** Group effects (z-scores relative to baseline) of changes in the variance of the accelerometer (Acc) after initial saline controls (last 10 min), DOI-M100907 or M100907 alone (min 25-35 after injections). **(B)** Group effects (z-scores) of changes in MUA in PFC and HPC. **(C)** Individual (one electrode) examples of changes in power over time after DOI-M100907 (upper panels) and the corresponding group effects (middle panels). Also shown are group effects after M100907 alone (lower panels). Black lines indicate the time of saline, DOI and M100907 administration. Mean Acc is also shown in red (in arbitrary units). Note the narrow 4 Hz band that emerges after M100907 (see also Supplementary Figure 3). **(D)** Quantification of changes in power (z-scores). **(E)** Quantification of changes in phase-lag index (PLI) (z-scores). Note the larger scale of DOI+M100907 plots compared to M100907 alone, an indication that M100907 exerted more prominent effects after DOI than when administered alone.

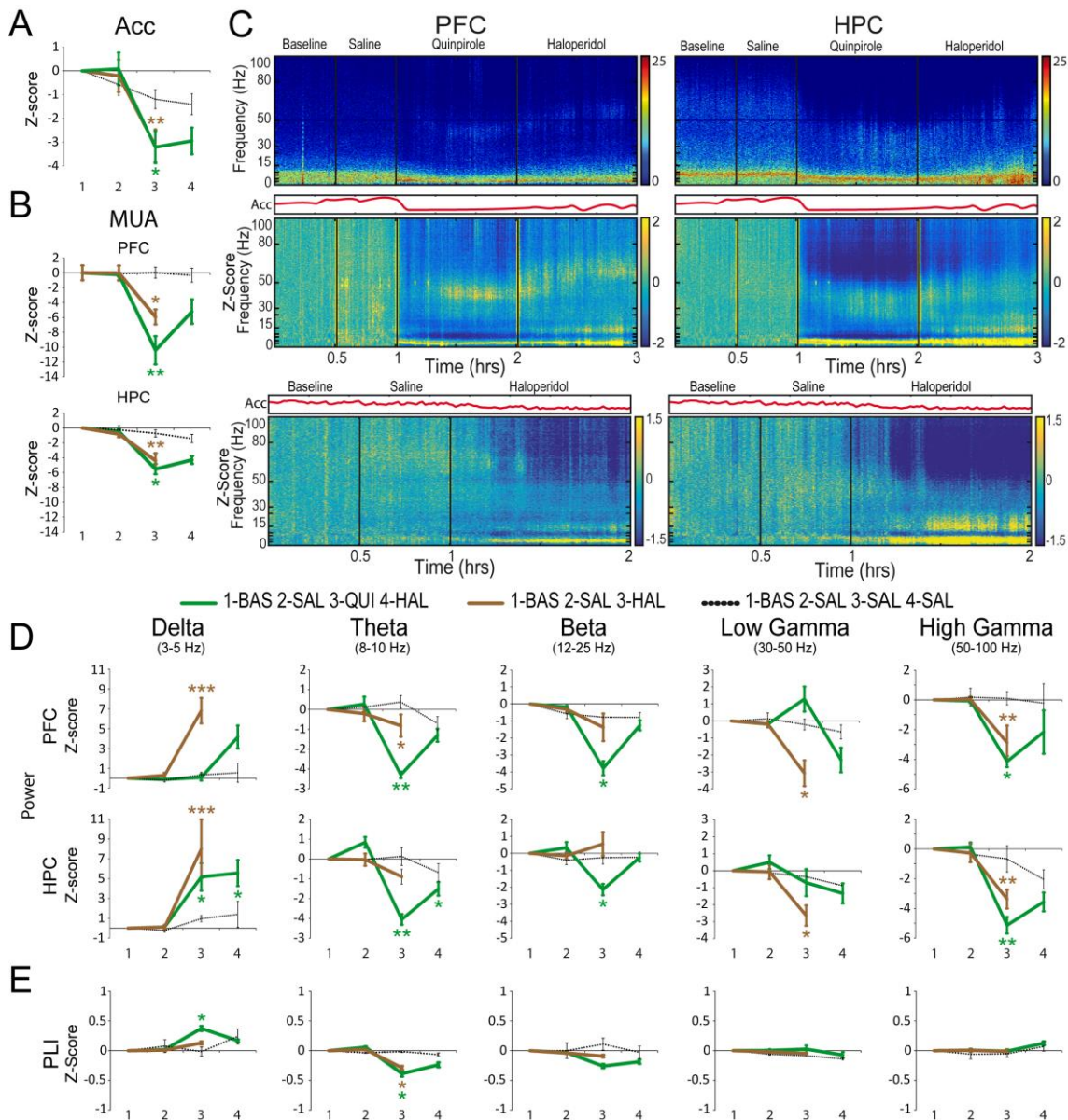


Figure 4. Activation and inhibition of D₂R with quinpirole (QUI; n = 4 mice) and haloperidol (HAL; n = 7 mice), respectively, reduce locomotion, MUA, power of theta and high gamma oscillations in PFC and HPC and PFC-HPC theta phase synchronization. Quinpirole also amplifies HPC delta waves and PFC-HPC delta phase synchronization while haloperidol increases delta and diminishes low gamma in both structures. **(A)** Group effects (z-scores relative to baseline) of changes in the variance of the accelerometer (Acc) after quinpirole-haloperidol or haloperidol alone (min 25-35 after injections). **(B)** Group effects (z-scores) of changes in MUA in PFC and HPC. **(C)** Individual (one electrode) examples of changes in power over time after quinpirole-haloperidol (upper panels) and group effects for quinpirole-haloperidol and haloperidol alone (lower panels). Black lines indicate time of saline, quinpirole and haloperidol administration. Mean Acc is also shown in red (in arbitrary units). **(D)** Quantification of changes in power (z-scores). **(E)** Quantification of changes in phase-lag index (PLI) (z-scores).

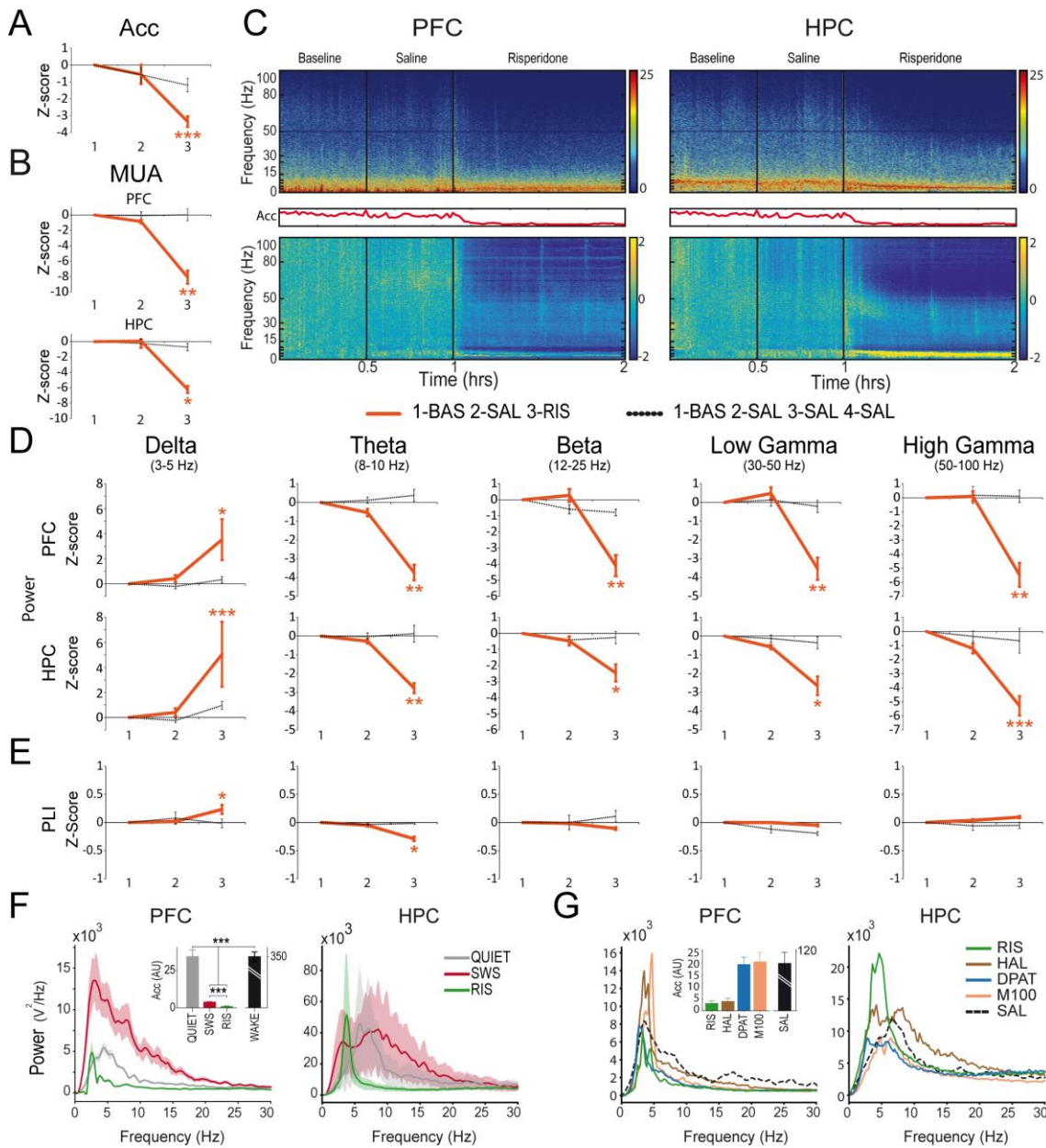


Figure 5. Risperidone (RIS; $n = 8$ mice) reduces locomotion, MUA, power of theta, beta, low gamma and high gamma oscillations in PFC and HPC and PFC-HPC theta phase synchronization. It also exacerbates delta oscillations and PFC-HPC delta phase synchronization. **(A)** Group effects (z-scores) of changes in the variance of the accelerometer (Acc) after RIS (min 25-35 after injections). **(B)** Group effects (z-scores) of changes in MUA in PFC and HPC. **(C)** Group effects (z-scores) for power changes (lower panels). Black lines indicate time of saline and RIS administration. Mean Acc is also shown in red (in arbitrary units). **(D)** Quantification of changes in power (z-scores) at relevant frequency bands. During sedative states there is a more pronounced suppression of locomotor activity than during quiet wakefulness (QUIET) and slow-wave sleep (SWS), and a narrow 4 Hz band emerges in PFC that is different from slow waves. **(E)** Quantification of changes in phase-lag index (PLI) (z-scores). **(F)** Power spectra and corresponding Acc of high-immobility episodes during quiet wakefulness (QUIET), slow-wave sleep (SWS), and RIS in PFC and HPC of one mouse. Normal locomotor activity during wakefulness (WAKE) has been added for reference. **(G)** Power spectra and corresponding Acc of high-immobility episodes after administration of drugs (all mice tested have been included). Note that serotonergic compounds elicit less locomotor activity suppression than APDs.

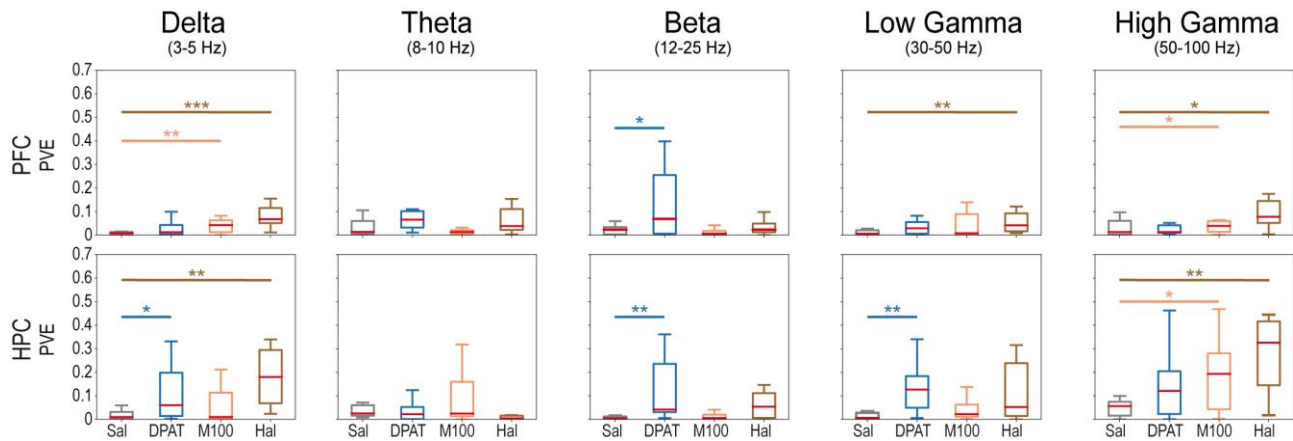


Figure 6. Linear regression models highlight 5-HT_{1A}R-like, 5-HT_{2A}R-like and D₂R-like actions of risperidone. Shown is the proportion of partial variance explained (PVE) for the drug effects only (see the estimated contribution of the animal's instantaneous acceleration alone in Supplementary information). Regressors: DPAT, M100907 (M100), haloperidol (HAL) and saline; regressand: RIS (Model 1: RIS vs. saline, n = 11 electrodes; model 2: RIS vs. DPAT, n = 10; Model 3: RIS vs. M100907, n = 15; Model 4: RIS vs. haloperidol, n = 15). In each model, the first regressor is sampled with non-overlapping LFP power estimates from the first hour following administration of DPAT, M100907, haloperidol or saline, respectively, in the same electrodes used to obtain LFP power samples under risperidone action. The second regressor is the variance of the animal's instantaneous acceleration during risperidone action. * $p < .05$, ** $p < .01$, *** $p < .001$, Wilcoxon Rank test.

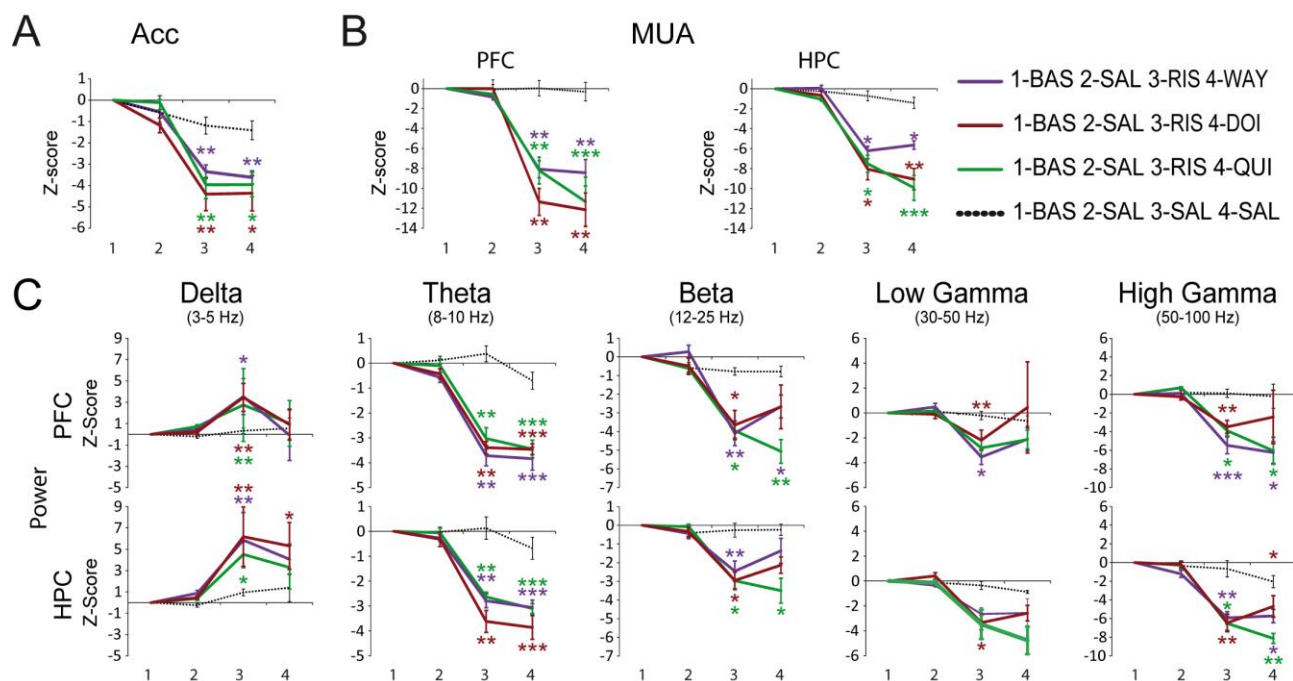


Figure 7. Risperidone modulates PFC-HPC network activity combining 5-HT_{1A}R, 5-HT_{2A}R and D₂R activities. The reversal treatments (WAY, DOI, QUI) are unable to normalize risperidone-induced reductions of locomotion, MUA and theta oscillations. However, they fully or partially reverse the effects of RIS depending of brain region and frequency band. **(A)** Group effects (z-scores with respect to baseline) of changes in the variance of the accelerometer (Acc) after RIS-WAY, RIS-DOI, RIS-QUI and saline controls (min 25-35 after injections). **(B)** Group effects (z-scores) of changes in MUA in PFC and HPC. **(C)** Group effects (z-scores) of changes in power.